THE UNIVERSITY of EDINBURGH

Edinburgh Research Explorer

Bidimensional Distribution Entropy to Analyze the Irregularity of Small-sized Textures

Citation for published version:
Azami, H, Escudero, J & Humeau-Heurtier, A 2017, 'Bidimensional Distribution Entropy to Analyze the Irregularity of Small-sized Textures', *IEEE Signal Processing Letters*, vol. 24, no. 9, pp. 1338-1342. https://doi.org/10.1109/LSP.2017.2723505

Digital Object Identifier (DOI):
10.1109/LSP.2017.2723505

Link:
Link to publication record in Edinburgh Research Explorer

Document Version:
Peer reviewed version

Published In:
IEEE Signal Processing Letters

General rights
Copyright for the publications made accessible via the Edinburgh Research Explorer is retained by the author(s) and / or other copyright owners and it is a condition of accessing these publications that users recognise and abide by the legal requirements associated with these rights.

Take down policy
The University of Edinburgh has made every reasonable effort to ensure that Edinburgh Research Explorer content complies with UK legislation. If you believe that the public display of this file breaches copyright please contact openaccess@ed.ac.uk providing details, and we will remove access to the work immediately and investigate your claim.

OPEN ACCESS

Download date: 12. Oct. 2024

Bidimensional Distribution Entropy to Analyze the Irregularity of Small-sized Textures

Hamed Azami[1,*], *Student Member*, *IEEE*, Javier Escudero[1], *Member*, *IEEE*, and Anne Humeau-Heurtier[2]

***Abstract*—Two-dimensional sample entropy (SampEn$_{2D}$) has been recently proposed to quantify the irregularity of textures. However, when dealing with small-sized textures, SampEn$_{2D}$ may lead to either undefined or unreliable values. Moreover, SampEn$_{2D}$ is too slow for most real-time applications. To alleviate these deficiencies, we introduce bidimensional distribution entropy (DistrEn$_{2D}$). We evaluate DistrEn$_{2D}$ on both synthetic and real texture datasets. The results indicate that DistrEn$_{2D}$ can detect different amounts of white Gaussian and salt and pepper noise, and discriminate periodic from synthesized textures. The results also show that DistrEn$_{2D}$ distinguishes different kinds of textured surfaces. In addition, DistrEn$_{2D}$, unlike SampEn$_{2D}$, does not lead to undefined values. Moreover, DistrEn$_{2D}$ is noticeably faster than SampEn$_{2D}$. Overall, DistrEn$_{2D}$ - as an insensitive feature extraction method to rotation - is expected to be very useful for the analysis of real image textures.**

***Index Terms*—Image processing, texture analysis, irregularity, bidimensional dispersion entropy, two-dimensional sample entropy.**

I. Introduction

In the field of signal processing, the interest brought to algorithms aiming at exploring the irregularity of signals is increasing. This can be observed by listing the new entropy-based algorithms that have recently been proposed to improve and extend one of the most well-known irregularity measures, sample entropy (SampEn$_{1D}$) [1]: see, e.g., [2]–[6]. This growing interest is probably due to the ability of the entropy-based algorithms to analyze large sets of signals [3] and also to their ability - when associated with a multiscale approach - to give information on the system's complexity [3], [7]. Among these recent methods, distribution entropy (DistrEn$_{1D}$) showed good performances when applied to both synthetic and experimental data [5]. Moreover, DistrEn$_{1D}$, unlike SampEn$_{1D}$, has low sensitivity to the parameters. The DistrEn$_{1D}$-based results also showed the stability of profiles even for short signals, which is not observed with SampEn$_{1D}$ [5].

However, in the field of image processing, to the best of our knowledge, only two algorithms have been proposed to analyze image irregularity [8], [9]. Nevertheless, the potential applications for irregularity measures in image processing is wide: image irregularity could be of great interest for texture analysis [8]–[10].

Based on the advantages of DistrEn$_{1D}$ over SampEn$_{1D}$ for short signals, we here introduce bidimensional distribution entropy (DistrEn$_{2D}$) to quantify the irregularity of texture images. Then, we compare the performance of DistrEn$_{2D}$ with the one given by the extension of SampEn$_{1D}$ to the 2D-case (SampEn$_{2D}$) [8]. For this purpose, the two algorithms are applied to small-sized synthetic textures. In addition, we use real textured surfaces to demonstrate the ability of DistrEn$_{2D}$ to distinguish different kinds of textures.

II. Bidimensional Distribution Entropy

Assume an image of size $h \times w$: $\mathbf{U} = \{u_{i,j}\}_{i=1,2,\dots,h}^{j=1,2,\dots,w}$. We define the algorithm of DistrEn$_{2D}$ as follows:

1) After normalizing $\mathbf{U}$ to the range of 0 to 1, all two-dimensional matrices $\mathbf{X}_{k,l}^{\mathbf{m}}$, ($k = 1, 2, ..., h - (m_h - 1)$ and $l = 1, 2, ..., w-(m_w-1)$) with size $m_h \times m_w$, named template matrices, are created, as shown in Eq. (1) on the top of the next page, where $\mathbf{m} = [m_h, m_w]$ denotes the embedding dimension vector.

2) We calculate the distance matrix $\mathbf{D} = \{d_{k,l}\}_{k=1,\dots,h-(m_h-1)}^{l=1,\dots,w-(m_w-1)}$, as the greatest element of the absolute difference of $\mathbf{X}_{k,l}^{\mathbf{m}}$ and $\mathbf{X}_{a,b}^{\mathbf{m}}$, where a and b change from 1 to $h-(m_h-1)$ and 1 to $w-(m_w-1)$, respectively. To reduce bias, elements with $(a, b) = (k, l)$ are not considered.

3) We employ the histogram approach with M bins to estimate the empirical probability density function (ePDF) of $\mathbf{D}$. We use p_t ($t = 1, \dots, M$) to denote the probability (frequency) of each bin.

4) Finally, the DistrEn$_{2D}$ of image $\mathbf{U}$ based on the Shannon's definition of entropy [11] is calculated as follows:

$$DistrEn_{2D}(\mathbf{U}, \mathbf{m}, M) = -\sum_{t=1}^{M} p_t \cdot \log_2(p_t). \qquad (2)$$

As DistrEn$_{2D}$ value changes from 0 to $\log_2(M)$, we use the normalized DistrEn$_{2D}$ as $\frac{1}{\log_2(M)} DistrEn_{2D}$ in this study. It is worth noting that DistrEn$_{2D}$ is insensitive to rotation as evidenced by the algorithm and also will be shown later.

There are two parameters for DistrEn$_{2D}$, namely the embedding dimension vector $\mathbf{m}$ and number of bins M in the histogram. For simplicity, like the recommendations for SampEn$_{2D}$ [8], we set $m_h = m_w = m$. The total number of elements in matrix $\mathbf{D}$ except its main diagonal is $TNE = (h-m+1)(w-m+1)((h-m+1)(w-m+1)-1)$, and this should then be the maximum value that M can be assigned. When $M > TNE$, the information underlying $\mathbf{D}$ cannot be appropriately quantified [5]. As $d_{k,l} = d_{l,k}$, $\mathbf{D}$ is symmetrical and so, the upper or lower triangular matrix will actually be enough for the estimation of the ePDF. Thus, we consider only a triangular part. In this study, we used the base-2 logarithm

[1] H. Azami and J. Escudero are with the Institute for Digital Communications, School of Engineering, The University of Edinburgh, Edinburgh, King's Buildings, EH9 3FB, United Kingdom. *Corresponding author (Phone: +44 7481478684; email: hamed.azami@ed.ac.uk).

[2] A. Humeau-Heurtier is with LARIS - Laboratoire Angevin de Recherche en Ingénierie des Systèmes, University of Angers, France.

$$\mathbf{X}^{\mathbf{m}}_{k,l} = \begin{bmatrix} u_{k,l} & u_{k,l+1} & \cdots & u_{k,l+(m_w-1)} \\ u_{k+1,l} & u_{k+1,l+1} & \cdots & u_{k+1,l+(m_w-1)} \\ \vdots & \vdots & \vdots & \vdots \\ u_{k+(m_h-1),l} & u_{k+(m_h-1),l+1} & \cdots & u_{k+(m_h-1),l+(m_w-1)} \end{bmatrix} \tag{1}$$

Fig. 1: Example of a reference image [13], sized 128×128, added with different levels of $\text{WGN}_{2\text{D}}$ and SPN.

in Eq. 2 to choose M as an integer of power 2. As we show later, $\text{DistrEn}_{2\text{D}}$ is not very sensitive to its parameter values. For $\text{SampEn}_{2\text{D}}$, we set r as 0.25 of the SD of an image [8].

III. Evaluation Images

In this section, we briefly describe the synthetic and real textures used in this study to assess the behaviour of $\text{DistrEn}_{2\text{D}}$.

1) *Two-dimensional MIX Process*: To assess the ability of $\text{DistrEn}_{2\text{D}}$ to detect different degrees of irregularity, we used two-dimensional MIX ($\text{MIX}_{2\text{D}}$) process [8] as follows:

$$\begin{aligned} MIX_{2D}(p)_{i,j} &= (1 - z_{i,j})x_{i,j} + z_{i,j}y_{i,j}, \\ i &= 1, 2, \ldots, h, \quad j = 1, 2, \ldots, w \end{aligned} \tag{3}$$

where $x_{i,j} = \sin(\frac{2\pi i}{12}) + \sin(\frac{2\pi j}{12})$, $\mathbf{Y} = \{y_{i,j}\}$ is a uniform two-dimensional matrix of white noise ($\text{WN}_{2\text{D}}$) ranged from $-\sqrt{3}$ to $\sqrt{3}$, and $z_{i,j}$ denotes a random variable which is equal to 1 with probability p and equals to 0 with probability $1 - p$ [8], [12]. Therefore, the larger the value of p, the more irregular the images.

2) *Texture Image with Additive Noise*: To show the dependency of $\text{DistrEn}_{2\text{D}}$ on white Gaussian noise ($\text{WGN}_{2\text{D}}$) and salt and pepper noise (SPN), we used a 128×128 texture, depicted in Fig. 1, from the Brodatz database [13]. Then, after normalizing the texture in the range 0 to 1, we added different levels of uniform $\text{WGN}_{2\text{D}}$ with mean 0.01, 0.05, and 0.09, and variance 0.01, 0.05, and 0.09, in that order. We also added SPN with different noise density values of 0.01, 0.05, and 0.09 to the reference normalized texture.

3) *Artificial Periodic and Synthesized Textures*: To show how $\text{DistrEn}_{2\text{D}}$ changes when a periodic texture turns into a synthesized texture, we employed four pairs of periodic and their corresponding synthesized textures from [14]. The original and their synthesized textures, sized 256×256, are depicted in Fig. 2(a) to (d), and Fig. 2(e) to (h), in that order.

4) Vision Textures: To show how $\text{DistrEn}_{2\text{D}}$ changes with increasing the degree of irregularity, we employed ten vision textures from [15]. The textures, sized 512×512, are shown in Fig. 3(a) to (j), ordered from least irregular (a) to most irregular (j) [16].

5) *Composite Textures*: We also employed four 256×256 composite texture images, used in [17]. Each image, shown in Fig. 4, includes five textures from the Brodatz database [13].

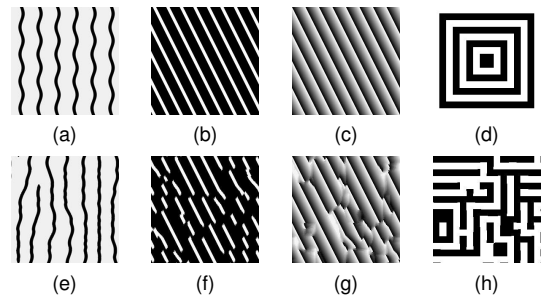

Fig. 2: Texture synthesis examples: (a), (b), (c), and (d) periodic textures and (e), (f), (g), and (h) their corresponding synthesized textures [14].

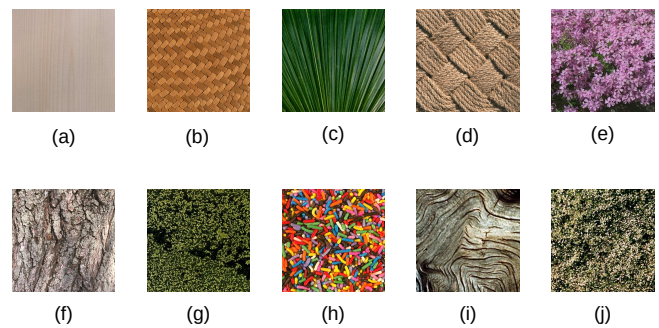

Fig. 3: Vision textures ordered from least irregular (a) to most irregular (j) [16].

6) *Textured Surfaces*: To evaluate the invariance properties of $\text{DistrEn}_{2\text{D}}$, we used a subset of a texture surface database including 200 uncalibrated, unregistered images: 40 samples each of 5 various textures, namely wood3, floor1, fur, brick1, and bark3. One sample of each of them is depicted in Fig. 5. The database, publicly available at [18], includes surfaces whose textures are due mainly to albedo variations (e.g., wood), 3D shape (e.g., fur), and a mixture of both (e.g., brick). Noticeable viewpoint changes and scale differences are observed within each class and illumination conditions are uncontrolled. During data acquisition, it has been paid attention to exercise further sources of variability wherever possible, including non-planarity of the textured surface (bark), significant non-rigid deformations between different samples of the same class (fur), and inhomogeneities of the texture pattern (bark). For more information, please refer to [19].

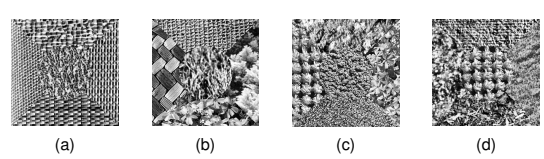

Fig. 4: Composite texture images used in our study [17].

Fig. 5: One sample of each of five various textured surfaces [18].

TABLE I: DistrEn_{2D} of (a), (b), (c), and (d) periodic textures and their (e), (f), (g), and (h) synthesized corresponding textures; see Fig. 2.

Texture (a)	Texture (b)	Texture (c)	Texture (d)
0.570	0.438	0.865	0.203
Texture (e)	Texture (f)	Texture (g)	Texture (h)
0.604	0.553	0.872	0.220

TABLE II: DistrEn_{2D} of vision textures, ordered from least irregular (a) to most irregular (j); see Fig. 3.

Texture (a)	Texture (b)	Texture (c)	Texture (d)	Texture (e)
0.515	0.715	0.738	0.786	0.797
Texture (f)	Texture (g)	Texture (h)	Texture (i)	Texture (j)
0.810	0.818	0.822	0.829	0.858

TABLE III: DistrEn_{2D} values of the composite texture images and their components; see Fig. 4.

Texture	Five components of a composite texture	Composite texture
(a)	0.849, 0.856, 0.859, 0.854, 0.832	0.861
(b)	0.842, 0.853, 0.828, 0.783, 0.840	0.864
(c)	0.841, 0.847, 0.841, 0.851, 0.839	0.857
(d)	0.843, 0.853, 0.797, 0.791, 0.841	0.856

IV. Results and Discussion

1) *Two-dimensional MIX Process*: To understand the effect of size of images, *m*, and *M* on DistrEn_{2D}, we created 40 different realizations of $\text{MIX}_{2D}(0.1)$, $\text{MIX}_{2D}(0.5)$, and $\text{MIX}_{2D}(0.9)$ which their sizes changed from 20×20 to 200×200, and *m* and *M* respectively change from 1 to 4 and 512 to 4096.

Fig. 6 shows the impact of different *M* and *r* values on respectively DistrEn_{2D} and SampEn_{2D}. Here, we set $m = 2$ for both metrics. The mean and standard deviation (SD) values of the results show that $\text{MIX}_{2D}(0.9)$ is more irregular than $\text{MIX}_{2D}(0.5)$, which is also more irregular than $\text{MIX}_{2D}(0.1)$, in agreement with [8]. However, as SampEn_{2D} counts matrix pairs in template matrices having $d[\mathbf{X}_{k,l}^{\mathbf{m},\mathbf{d}}, \mathbf{X}_{a,b}^{\mathbf{m},\mathbf{d}}] \leq r$, when the size of an image or threshold *r* is small, this number may be 0, leading to undefined values. Accordingly, the SampEn_{2D} values, unlike the DistrEn_{2D} ones, for various image sizes are undefined in Fig. 6, occurring in the cases where there is no output.

We also evaluate the effect of *m* on these approaches. The results, depicted in Fig. 7, follow the concept of irregularity for the MIX_{2D} process as the larger the value of *p*, the more irregular the image [8], [12]. However, a number of SampEn_{2D} values are undefined, especially for larger *m* or smaller image sizes. Overall, the entropy values for DistrEn_{2D} with different *m* and *M* are always defined, evidencing an advantage of DistrEn_{2D} over SampEn_{2D}.

2) *Texture Image with Additive Noise*: The results, depicted in Fig. 8, show that the additive WGN_{2D} of larger mean and variance leads to a higher entropy value. Moreover, adding SPN with larger noise density results in a higher entropy value. Both evidence that DistrEn_{2D} can detect different levels of WGN_{2D} and SPN. For simplicity, we set $m = 2$ and $M = 512$ for DistrEn_{2D} in all simulations below, although the ranges $256 \leq M \leq 4096$ and $1 \leq m \leq 5$ lead to similar results (data not shown).

3) *Artificial Periodic and Synthesized Textures*: Table I demonstrates that DistrEn_{2D} of a periodic texture is lower than that of its corresponding synthesized texture. This fact shows that DistrEn_{2D} may be of great interest to quantify the periodicity of images.

4) Vision Textures: The results, depicted in Table II, suggest that the more irregular the texture, the higher the DistrEn_{2D} value, showing that DistrEn_{2D} may be of great interest to quantify the degree of irregularity of textures.

5) *Composite Textures*: The results for four 256×256 composite texture images, shown in Table III, demonstrate that the DistrEn_{2D} value of each of the composite textures is higher than all the entropy values of its five components. It is in agreement with the fact that, in general, composing textures may derive more various patterns, leading to more irregularity and subsequently a higher entropy value. This fact also evidences that DistrEn_{2D} may be considered as a measure to quantify the irregularity of images.

6) *Textured Surfaces*: The DistrEn_{2D} values of 200 images of five different textures are shown in Table IV. The results show that there are no overlaps between entropy values of five different groups, evidencing that DistrEn_{2D} may be an appropriate feature extraction method to detect the dynamics of images to distinguish different kinds of textures or images.

7) *Sensitivity to Rotation of Images*: We employed Lenna as a standard widely-used image, sized 256×256, in the field of image processing and rotated it by 90, 180, and 270 degrees in a counterclockwise direction around its center point using bilinear interpolation. The DistrEn_{2D} of the original image (0.6615) is equal to that of each of the rotated images, evidencing DistrEn_{2D} is insensitive to the rotation of images, as it is clear in the DistrEn_{2D} algorithm.

V. Computation Time

To evaluate the computation time of DistrEn_{2D}, compared with the one of SampEn_{2D}, we created $\text{MIX}_{2D}(0.5)$ with different sizes changing from 50×50 to 300×300. The computation times are shown in Table IV. The simulations have been carried out by the use of a PC with Intel (R) Xeon (R) CPU, E5420, 2.5 GHz and 8-GB RAM by MATLAB R2015a. Table V shows that SampEn_{2D} with $m = 3$ is relatively faster than SampEn_{2D} with $m = 2$, and the latter one is comparatively faster than SampEn_{2D} with $m = 1$. However, the computation time for DistrEn_{2D} is not very sensitive to *m*. DistrEn_{2D} is about 20 and 2 times faster than SampEn_{2D} for the image with size 50×50 and 200×200, respectively. It is one reason that we stress the importance of DistrEn_{2D} for especially small-sized textures. Overall, DistrEn_{2D} is noticeably quicker than SampEn_{2D}, suggesting the superiority of DistrEn_{2D} over SampEn_{2D} especially for small-sized images.

VI. Conclusions

We introduced DistrEn_{2D} to quantify the irregularity of textures or images. The results showed the great ability of

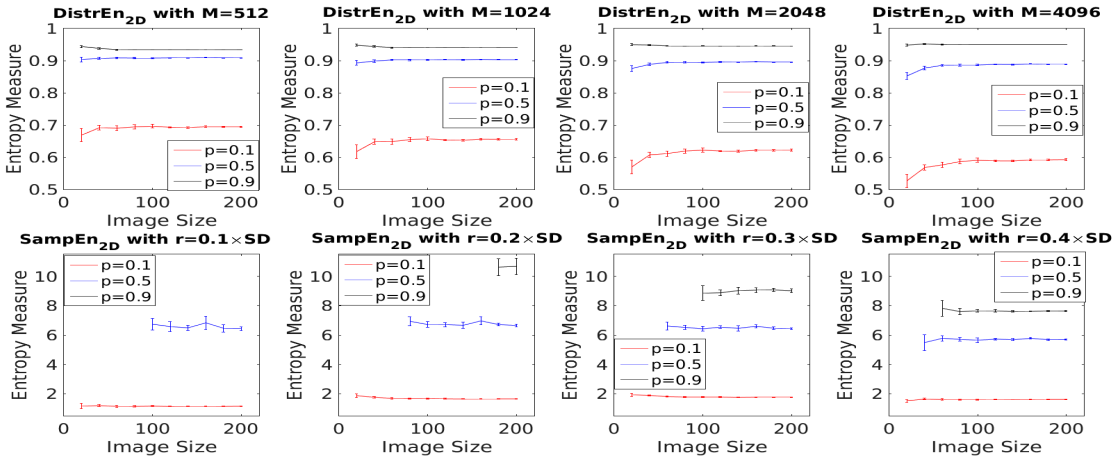

Fig. 6: Mean value and SD of results obtained by the DistrEn_{2D} and SampEn_{2D} computed from 40 different $\text{MIX}_{2D}(0.1)$, $\text{MIX}_{2D}(0.5)$, and $\text{MIX}_{2D}(0.9)$. Results are shown for different M (DistrEn_{2D}) and r (SampEn_{2D}) values.

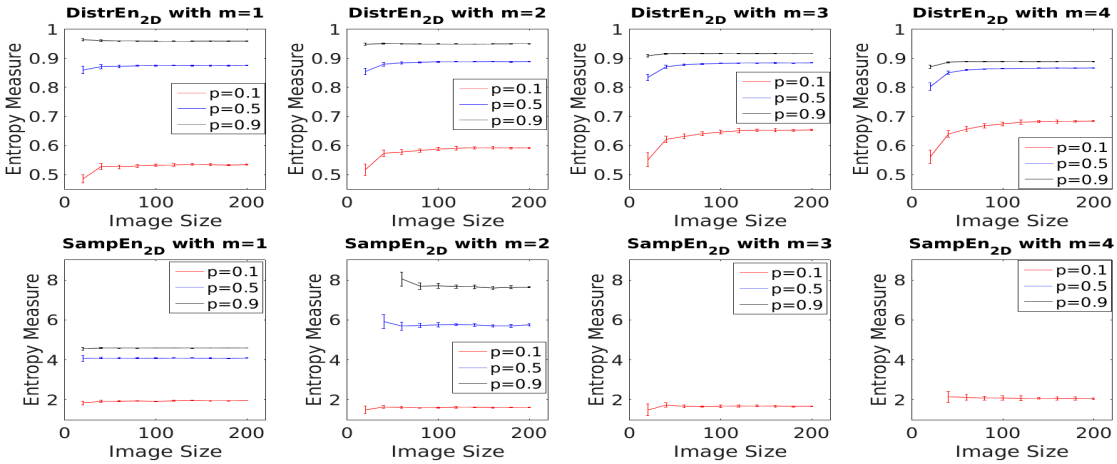

Fig. 7: Mean value and SD of results obtained by the DistrEn_{2D} and SampEn_{2D} computed from 40 different $\text{MIX}_{2D}(0.1)$, $\text{MIX}_{2D}(0.5)$, and $\text{MIX}_{2D}(0.9)$. Results are shown for different m values.

TABLE IV: DistrEn_{2D} of five different groups of textured surfaces shown as mean $\pm$ SD; see Fig. 5.

wood3	floor1	fur	brick1	bark3
0.714 ± 0.012	0.738 ± 0.005	0.757 ± 0.012	0.779 ± 0.010	0.816 ± 0.021

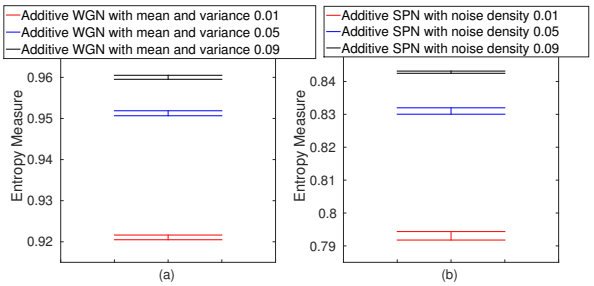

Fig. 8: Mean value and SD of results obtained by the DistrEn_{2D} computed from the reference image added with 40 realizations of different levels of (a) WGN_{2D} and (b) SPN.

TABLE V: Computational time of SampEn_{2D} and DistrEn_{2D}.

Image size $\rightarrow$	50×50	100×100	200×200	300×300
SampEn_{2D} (m=1)	2.829 s	48.134 s	798.116 s	4046.084 s
SampEn_{2D} (m=2)	2.046 s	36.421 s	605.542 s	3080.300 s
SampEn_{2D} (m=3)	1.872 s	34.117 s	566.594 s	2909.106 s
DistrEn_{2D} (m=1)	0.118 s	1.556 s	24.615 s	1497.366 s
DistrEn_{2D} (m=2)	0.109 s	1.580 s	25.610 s	1565.553 s
DistrEn_{2D} (m=3)	0.111 s	1.687 s	27.619 s	1583.193 s

DistrEn_{2D} to distinguish different amounts of WGN_{2D} and SPN, periodic from synthesized textures, and different types of textured surfaces. DistrEn_{2D} dealt with the problem of undefined SampEn_{2D} values for small-sized textures. We also demonstrated that DistrEn_{2D} is considered as an insensitive feature extraction method to image rotation. Additionally, DistrEn_{2D} is considerably faster than SampEn_{2D} especially for small-sized images. Accordingly, DistrEn_{2D} has great potential to analyze various textures. In future work, we will investigate the suitability of DistrEn_{2D} to characterize the variability of other real textures and images, such as [20], [21].

References

[1] J. S. Richman and J. R. Moorman, "Physiological time-series analysis using approximate entropy and sample entropy," *American Journal of Physiology-Heart and Circulatory Physiology*, vol. 278, no. 6, pp. H2039–H2049, 2000.

[2] A. Humeau-Heurtier, "The multiscale entropy algorithm and its variants: a review," *Entropy*, vol. 17, no. 5, pp. 3110–3123, 2015.

[3] A. Humeau-Heurtier, C.-W. Wu, and S.-D. Wu, "Refined composite multiscale permutation entropy to overcome multiscale permutation entropy length dependence," *IEEE Signal Processing Letters*, vol. 22, no. 12, pp. 2364–2367, 2015.

[4] M. Costa, A. L. Goldberger, and C.-K. Peng, "Multiscale entropy analysis of complex physiologic time series," *Physical Review Letters*, vol. 89, no. 6, p. 068102, 2002.

[5] P. Li, C. Liu, K. Li, D. Zheng, C. Liu, and Y. Hou, "Assessing the complexity of short-term heartbeat interval series by distribution entropy," *Medical & Biological Engineering & Computing*, vol. 53, no. 1, pp. 77–87, 2015.

[6] M. Rostaghi and H. Azami, "Dispersion entropy: A measure for time series analysis," *IEEE Signal Processing Letters*, vol. 23, no. 5, pp. 610–614, 2016.

[7] H. Azami, M. Rostaghi, D. Abasolo, and J. Escudero, "Refined composite multiscale dispersion entropy and its application to biomedical signals," *IEEE Transactions on Biomedical Engineering*, DOI: 10.1109/TBME.2017.2679136, 2017.

[8] L. Silva, A. Senra Filho, V. Fazan, J. Felipe, and L. M. Junior, "Two-dimensional sample entropy: assessing image texture through irregularity," *Biomedical Physics & Engineering Express*, vol. 2, no. 4, p. 045002, 2016.

[9] T. Marchant, M. Murphy, G. Madden, and C. Moore, "Quantifying structure regularity in fluorescence microscopy cell images using a novel multi-dimensional approximate entropy metric," in *Image Processing (ICIP), 2011 18th IEEE International Conference on*, pp. 3085–3088, IEEE, 2011.

[10] L. E. V. da Silva, A. C. da Silva Senra Filho, V. P. S. Fazan, J. C. Felipe, and L. O. Murta, "Two-dimensional sample entropy analysis of rat sural nerve aging," *Engineering in Medicine and Biology Society (EMBC), 36th Annual International Conference of the IEEE*, pp. 3345–3348, 2014.

[11] C. E. Shannon, "A mathematical theory of communication," *ACM SIGMOBILE Mobile Computing and Communications Review*, vol. 5, no. 1, pp. 3–55, 2001.

[12] H. Azami and J. Escudero, "Improved multiscale permutation entropy for biomedical signal analysis: Interpretation and application to electroencephalogram recordings," *Biomedical Signal Processing and Control*, vol. 23, pp. 28–41, 2016.

[13] P. Brodatz, *Textures: a photographic album for artists and designers*. Dover Pubns, 1966.

[14] https://graphics.stanford.edu/projects/texture/demo/synthesis_eero.html.

[15] http://vismod.media.mit.edu/vismod/imagery/VisionTexture/vistex.html.

[16] G. Ciocca, S. Corchs, and F. Gasparini, "Complexity perception of texture images," in *International Conference on Image Analysis and Processing*, pp. 119–126, Springer, 2015.

[17] T. Randen and J. H. Husoy, "Filtering for texture classification: A comparative study," *IEEE Transactions on Pattern Analysis and Machine Intelligence*, vol. 21, no. 4, pp. 291–310, 1999.

[18] http://www-cvr.ai.uiuc.edu/ponce_grp/.

[19] S. Lazebnik, C. Schmid, and J. Ponce, "A sparse texture representation using local affine regions," *IEEE Transactions on Pattern Analysis and Machine Intelligence*, vol. 27, no. 8, pp. 1265–1278, 2005.

[20] H. Tamura, S. Mori, and T. Yamawaki, "Textural features corresponding to visual perception," *IEEE Transactions on Systems, Man, and Cybernetics*, vol. 8, no. 6, pp. 460–473, 1978.

[21] A. D. Clarke, F. Halley, A. J. Newell, L. D. Griffin, and M. J. Chantler, "Perceptual similarity: A texture challenge.," in *BMVC*, pp. 1–10, 2011.